Development of a phantom mimicking the functional and structural behaviors of the thigh muscles characterized with magnetic resonance elastography technique

Mashhour Chakouch, Fabrice Charleux, Sabine F Bensamoun

Development of a phantom mimicking the functional and structural behaviors of the thigh muscles characterized with magnetic resonance elastography technique

Mashhour K. Chakouch, *Member, IEEE,* Fabrice Charleux, Sabine F. Bensamoun

***Abstract*— Magnetic Resonance Elastography (MRE) is a non invasive technique based on the propagation of shear waves in soft tissues providing the quantification of the mechanical properties [1]. MRE was successfully applied to healthy and pathological muscles. However, the MRE muscle methods must be further improved to characterize the deep muscles. A way will be to develop phantom mimicking the muscle behavior in order to set up new MRE protocol. Thus, the purpose of this study is to create a phantom composed of a similar skeletal muscle architecture (fiber, aponorosis) and equivalent elastic properties as a function of the muscle state (passive or active). Two homogeneous phantoms were manufactured with different concentrations of plastisol to simulate the elastic properties in relaxed (50% of plastisol) and contracted (70% of plastisol) muscle conditions. Moreover, teflon tubing pipes (D = 0.9 mm) were thread in the upper part of the phantom (50%) to represent the muscle fibers and a plastic sheet (8 x 15 cm) was also included in the middle of the phantom to mimic the aponeurosis structure. Subsequently, MRE tests were performed with two different pneumatic drivers, tube and round, (f = 90Hz) to analyze the effect of the type of driver on the wave propagation. Then, the wavelength was measured from the phase images to obtain the elastic properties (shear modulus). Both phantoms revealed elastic properties which were in the same range as in vivo muscle in passive ($\mu_{50\%}$ = 2.40 ± 0.18 kPa) and active (6.24 ± 0.21 kPa) states. The impact of the type of driver showed higher values (about 1.2kPa) with the tube. The analysis of the wave behavior revealed a sliding along the plastic sheet as it was observed for in vivo muscle study. The wave was also sensitive to the presence of the fibers where gaps were identified. The present study demonstrates the ability of the phantom to mimic the structural and functional properties of the muscle.**

I. Introduction

Palpation is one of the methods that the clinician used to detect abnormal changes of stiffness in soft tissue [2]. However, palpation is subjective and deep lesions are often unreachable. Biopsy is always the reference method in detecting abnormal tissue changes, revealed by mechanical modifications. Nevertheless, biopsy remains invasive and painful method providing an analysis of a small piece of target tissue (local measurement). Thus, the non-invasive evaluation of the functional properties of soft tissues is a key points for the clinicians to evaluate the behaviors of various tissues (muscle, brain, kidney, prostate, breast, and liver) before and after treatment.

MRE (Magnetic Resonance Elastography) is a non-invasive medical imaging technique which can quantify *in vivo* tissue stiffness by analyzing the propagation of shear waves through soft tissues [3]. This method is increasingly used in clinical practice for liver diagnostic purpose [4] and is further developed to assess the mechanical properties of the brain, heart and skeletal muscles [4]–[8]. A way to contribute to MRE protocol improvement is the development of phantoms that realistically simulate the mechanical properties of soft tissues. In the field of radiology, phantom means any object mimicking the physical properties of human tissues, which are used for calibration and control imaging (MRI, CT, US) machines.

In the literature, phantoms were made with different compositions (agarose [9], bovine [10], wirosil® [11], plastisol® [12], zerdine hydrogel [13]) to test MRE parameters (voltage, frequency,…). MRE technique provided the viscoelastic properties of the phantoms which were usually validated with other mechanical techniques such as rheometers or dynamic mechanical analyses (*DMA)*. MRE was also combined with diffusion tensor imaging to determine the anisotropic properties of in vitro [14] and in vivo muscle tissue [15].

One of the main challenges of MRE technique applied to thigh muscle is the characterization of the deep muscles. Thus, the purpose of this study is to develop a phantom composed of similar skeletal muscle architecture (fiber, aponeurosis) and equivalent elastic properties as a function of the muscle state (passive or active). This new phantom will help to the development of new MRE muscle protocol. Thus, in vitro muscle MRE tools (type of drivers, coils, …) and MRE parameters (frequency, TR, TE,…) could be tested before to be in vivo applied.

II. Materials and Methods

A. Development of phantoms with similar muscle elastic properties

Previously, we have determined the elastic properties of relaxed and contracted muscles [16]. The objective was to develop an homogeneous media with equivalent stiffness in for both conditions. Thus, the phantoms were made with a mixture of softener and liquid plastic (LureCraft, LaGrande, USA), or plastisol, which is a suspension of PVC (polyvinyl chloride) particles in a plasticizer. Two homogeneous phantoms were manufactured with different concentrations (%) of plastisol in order to represent the relaxed (50%) (Fig.

*Research supported by Sorbonne University, Université de Technologie de Compiègne.

M.K.Chakouch, S.F. Bensamoun are with the UMR CNRS 7338 - Biomechanics and Bioengineering, Sorbonne University, University of Technology of Compiègne, BP 20529, 60205 Compiègne cedex, France (Corresponding author: 33 3 44 23 43 90/ sabine.bensamoun@utc.fr).

F. Charleux is with ACRIM-Polyclinique St Côme, BP 70409 - 60204, Compiègne Cedex, France.

1A) and contracted (70%) (Fig. 1B) muscle. Subsequently, both mixtures were heated to 177 °C [12], pour into cylindrical metal molds (19 x 15 cm), and left to cool at the room temperature (23°C) until the phantoms were solidified. They were stocked and preserved at the room temperature (23°C).

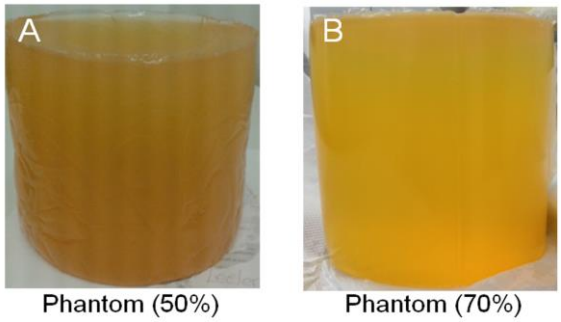

Figure 1. A-B: Phantoms mimicking the muscle in passive (A) and active (B) states.

B. *Development of phantom with similar muscle architecture*

The thigh is composed of surperficial muscles (RF, Fig. 2A) and deep muscles (such as VI, Fig. 2A), made of muscle fibers, and separated with aponeurosis membrane. To simulate the muscle fibers, teflon tubing pipe (internal diameter: 0.6 mm, external diameter: 0.9 mm) were thread in the upper part of the phantom, having 50% of plastisol. To mimick the aponeurosis, a plastic sheet (8 x 15 cm) was included in the middle of the phantom (Fig. 2B).

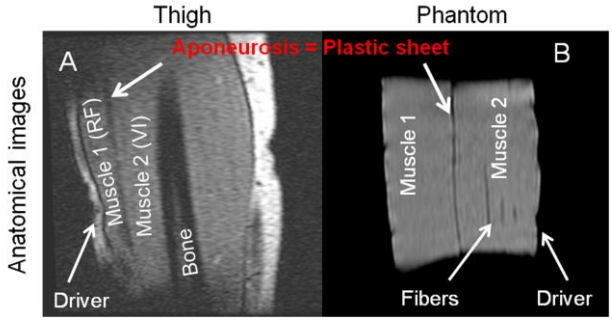

Figure 2. MRI sagittal acquisitions of the thigh muscles (RF: Rectus femoris, VI: Vastus intermedius) (A) and the phantom (50%) (B).

C. *MRE test performed on the phantom mimicking the muscle architecture in a passive condition*

MRE tests were conducted on the phantom composed of 50% plastisol, within a 1.5T MRI machine (General Electric HDxt). The phantom was placed with the fibers oriented in the same direction as in vivo muscle MRE test. To generate the waves within the phantom, two different pneumatic drivers were used (Fig. 3) to analyze the effect of the driver on the wave propagation. The first one was the same silicone tube used for in vivo muscle and the second one has a round shape, and is used in clinical practice for liver analysis. The tube driver was wrapped and clamped around one extremity of the phantom (Fig. 3A) simulating the in vivo placement of the tube at the end of the distal part of the thigh [3]. The tambour driver was placed below and above the phantom (Fig. 3B). A long hose was connected to a large active loudspeaker to send the air pressure at the optimal in vivo muscle frequency (f: 90 Hz). The MR acquisitions were recorded with the body coil.

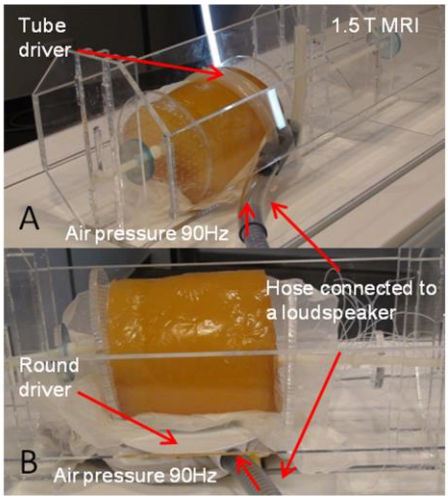

Figure 3. MRE Experimental set-up for the phantom with both drivers

D. *Image processing and data analysis*

Phase images, revealing the propagation of the shear waves, were recorded for the phantom (Fig. 4A-B), and the muscle (Fig. $6C_1$) [8]. A post-processing was applied with a mask, removing the noise located in the background of the image. Butterworth filter was also applied to suppress interfering wave patterns.

The elastic properties (shear modulus: μ) were measured from the displacement of the shear wave visualized on the phase images. Assuming that the media is linear elastic, isotropic, homogeneous and incompressible, the shear modulus (μ) was calculated using the following equation $\mu = \rho . (f . \lambda)^2$, where ρ is the muscle density fixed to 1000 kg/m^3. The behavior of the wavelength (λ) was represented through a profile manually prescribed in the direction of the shear wave propagation within the phantom (Fig. 4A-B).

III. Results

A. *Elastic properties of the phantoms as a function of:*

1) *The concentration of plastisol*

Figure 4A-B showed the recorded phase images, obtained for the homogeneous phantoms (without fiber) composed of 50% and 70% of plastisol concentration. A clear visualization of the wave propagation was observed within the phantoms. An increase of the wavelength (λ) was obtained when the plastisol concentration was increased (Fig. $4A_1$-B_1). The shear modulus measurements for the phantoms at 50% and 70% of plastisol were $\mu_{50\%} = 2.40 \pm 0.18$ kPa and $\mu_{70\%} = 6.24 \pm 0.21$ kPa, respectively. These elastic properties were in agreement with our previous study performed on passive ($\mu = 3.83 \pm 0.24$ kPa) and active ($\mu = 7.33 \pm 1.23$ kpa) thigh muscle [17].

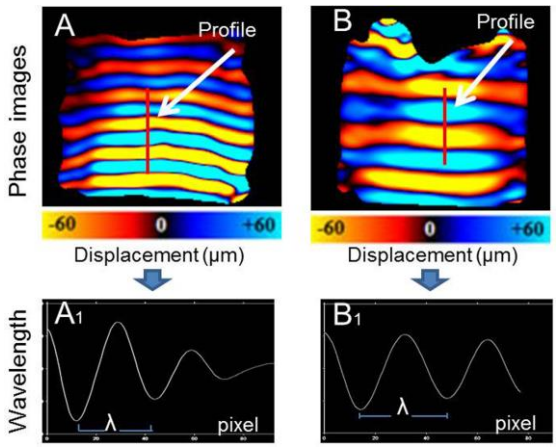

Figure 4. A-B: MRE tests were performed on both phantoms with a round driver and showed the wave's displacement inside both media. A_1-B_1: Behaviors of the waves traveling along the red profile.

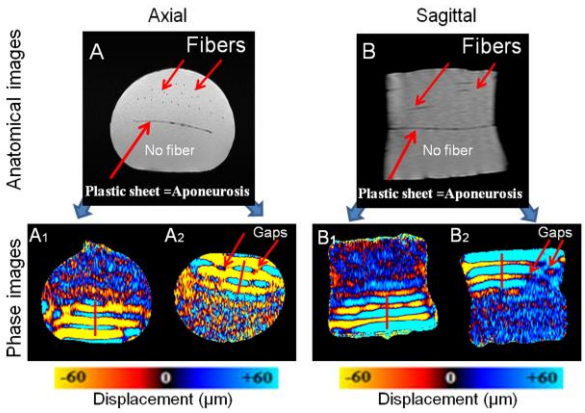

Figure 5. A-B: Axial and sagittal anatomical images of the phantom (50%) where the fibers inclusions are localized. Phase images obtained through MRE experiments performed at 90Hz with the tambour driver in contact with the sides without inclusion (A1-B1) and with inclusion (A2-B2).

2) The type of drivers

Different drivers were tested on the phantom (50%) in order to analyze the impact of the driver on the shear wave displacement. Figure 5 and Figure 6 showed the results of the phase images, acquired through axial and sagittal scan plans, using the round pneumatic and the silicone tube drivers (f: 90Hz), respectively.

Using the round driver (Fig. 5), the shear modulus measured, along the red profile, on the axial ($\mu_{\_axial}$ = 2.94 ± 0.18 kPa) and sagittal ($\mu_{\_sagittal}$ = 3.04 ± 0.21 kPa) plans were in the same range.

Using the tube driver (Fig. 6), the shear modulus measured on the axial ($\mu_{\_axial}$ =4.47± 0.51 kPa) image was approximately the same as for the one measured through the sagittal plan ($\mu_{\_sagittal}$ = 4.24 ± 0.25 kPa).

It can be concluded that for each driver, the same range of stiffness was found with axial and sagittal acquisitions. This result demonstrated the homogeneity of the phantom.

The comparison of the shear modulus obtained with both drivers showed an effect of the type of driver on the stiffness value. Indeed, higher values (range: 1.2 kPa to 1.53 kPa) were found with the tube driver.

B. *Characterization of the shear wave behavior*

Figure 5 showed the results of the shear wave displacement when the round driver was placed below (Fig. $5A_1$-B_1) and above (Fig. $5A_2$-B_2) the phantom. It can be noted that the shear wave did not pass through the plastic sheet which plays the role of aponeurosis.

The same result was obtained with the tube driver (Fig. $6B_1$), and a sliding of the wave along the plastic sheet was also visualized. The same phenomena occurred for in vivo muscle study (Fig. $6C_1$).

For both drivers, a uniform propagation was observed in the part without inclusion. However, the wave behavior was sensitive to the presence of the fibers. Gaps were identified in the fiber side (Fig. $5A_2$-B_2 and Fig. $6A_1$-B_1). Similar shear modulus was found between both sides due to the unload fibers.

The tube driver generated the waves all around the phantom and Fig. $6A_1$ revealed a uniform repartition of the vibration within the tube. At the opposite, a local source of the vibration was provided with the round driver which must be moved as a function of the investigated area.

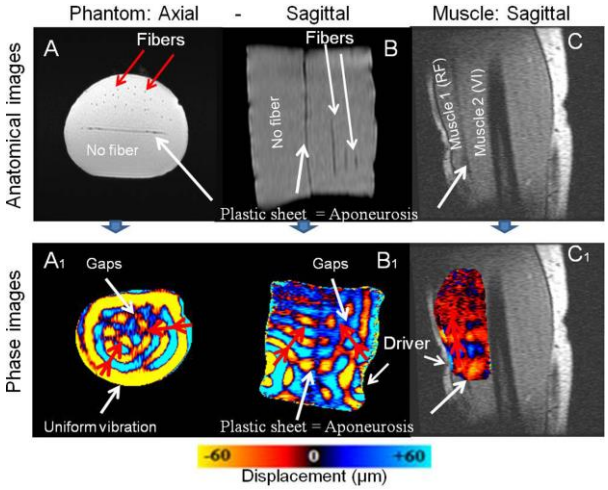

Figure 6. A-B-C: Views of the axial and sagittal anatomical images of the phantom (50%) and muscle (C). A_1-B_1: Result of the MRE experiments performed with the tube driver attached around the phantom. C_1: MRE tests were previousely performed [8] with a silicone tube driver on the selected sagittal image leading to the acquisition of in vivo phase images. Wave direction indicated by arrows along the red profile.

IV. Discussion

MRE has been extensively developed to characterize the functional properties of biological soft tissues such as liver [4] providing fibrosis diagnosis. Further experiments are now performed on muscle tissue to evaluate the effect of treatment in case of muscle pathology [18]. In comparison to the liver tissue, skeletal muscle is a physiological complex material, with a hierarchical organization, anisotropic and non-linear behaviors acting in passive and active states.

Thus, it was necessary to develop a realistic phantom mimicking the same structural and functional properties as the muscle tissue. The characterization of the surface muscles is easier compared to the deep ones which are

unreachable. Thus, the present phantom will allow to test different drivers to improve the deep propagation of the wave, and other MRE parameters to develop an optimal protocol as a function of the target muscle. The comparison between in vivo and in vitro (Fig. $6B_1$- C_1) studies showed a similar behavior of the wave displacement which did not pass through the muscle membrane. It will be also of interest to analyze the effect of the fiber orientation on the wave displacement. Moreover, equivalent shear moduli were found between in vivo and in vitro study using the tube driver, usually used for in vivo MRE muscle test. These results revealed that the present phantom could be a suitable object to set up new protocols for the deep muscles.

It can be noted that the phantom was placed in a device adapted to stretch the fibers at different levels. A stress muscle could be therefore simulated with the same developed phantom. This test object will be further developed with surrounded environmental tissue such as the adipose tissue. In a previous study, we have determined the elastic properties of this tissue and by adjusting the plastic concentration level it will be possible to also simulate this material. Moreover, the fibrosis tissue identified within pathological muscle (Duchenne, myopathy) [19] could be also incorporated within the present phantom. Indeed, we have previously measured a stiffer media in Duchenne muscle in passive condition. However, the displacement of the wave was difficult to follow due to this muscle composition. Thus, the phantom could help to better interpret the changes of the wave behavior within myopathic muscle which are composed of broken muscle fibers and fibrosis infiltration. This artificial muscle, represented by the phantom, will help to develop a new MRE protocol optimized for this type of myopathy.

V. Conclusion

The present study demonstrated the ability of the present phantom to mimic the composition (fiber, …) and the passive mechanical properties of the muscle. Another challenging way would be to incorporate the viscosity of the muscle to have the real viscoelastic behavior of this tissue.
This study is a first step toward an artificial muscle allowing the development of in vitro MRE protocol, to mimic healthy and pathological muscles, before to perform the in vivo MRE tests.

References

[1] R. Muthupillai, D. Lomas, P. Rossman, J. Greenleaf, A. Manduca, and R. Ehman, “Magnetic resonance elastography by direct visualization of propagating acoustic strain waves,” *Science*, vol. 269, no. 5232, pp. 1854–1857, Sep. 1995.

[2] J. Palacio-Torralba, S. Hammer, D. W. Good, S. Alan McNeill, G. D. Stewart, R. L. Reuben, and Y. Chen, “Quantitative diagnostics of soft tissue through viscoelastic characterization using time-based instrumented palpation,” *J. Mech. Behav. Biomed. Mater.*, vol. 41, pp. 149–160, Jan. 2015.

[3] S. F. Bensamoun, S. I. Ringleb, L. Littrell, Q. Chen, M. Brennan, R. L. Ehman, and K.-N. An, “Determination of thigh muscle stiffness using magnetic resonance elastography,” *J. Magn. Reson. Imaging*, vol. 23, no. 2, pp. 242–247, Feb. 2006.

[4] G. E. Leclerc, F. Charleux, L. Robert, M.-C. Ho Ba Tho, C. Rhein, J.-P. Latrive, and S. F. Bensamoun, “Analysis of liver viscosity behavior as a function of multifrequency magnetic resonance elastography (MMRE) postprocessing,” *J. Magn. Reson. Imaging*, p. n/a–n/a, 2013.

[5] J. Guo, S. Hirsch, A. Fehlner, S. Papazoglou, M. Scheel, J. Braun, and I. Sack, “Towards an Elastographic Atlas of Brain Anatomy,” *PLoS ONE*, vol. 8, no. 8, p. e71807, Aug. 2013.

[6] L. Huwart, F. Peeters, R. Sinkus, L. Annet, N. Salameh, L. C. ter Beek, Y. Horsmans, and B. E. Van Beers, “Liver fibrosis: non-invasive assessment with MR elastography,” *NMR Biomed.*, vol. 19, no. 2, pp. 173–179, 2006.

[7] M. A. Green, L. E. Bilston, and R. Sinkus, “In vivo brain viscoelastic properties measured by magnetic resonance elastography,” *NMR Biomed.*, vol. 21, no. 7, pp. 755–764, Aug. 2008.

[8] M. K. Chakouch, F. Charleux, and S. F. Bensamoun, “New magnetic resonance elastography protocols to characterise deep back and thigh muscles.,” *Comput. Methods Biomech. Biomed. Engin.*, vol. 17 Suppl 1, pp. 32–33, 2014.

[9] T. Numano, Y. Kawabata, K. Mizuhara, T. Washio, N. Nitta, and K. Homma, “Magnetic resonance elastography using an air ball-actuator,” *Magn. Reson. Imaging*, vol. 31, no. 6, pp. 939–946, Jul. 2013.

[10] Q. Chen, S. Bensamoun, J. R. Basford, J. M. Thompson, and K.-N. An, “Identification and Quantification of Myofascial Taut Bands With Magnetic Resonance Elastography,” *Arch. Phys. Med. Rehabil.*, vol. 88, no. 12, pp. 1658–1661, Dec. 2007.

[11] A. Kolipaka, K. P. McGee, A. Manduca, A. J. Romano, K. J. Glaser, P. A. Araoz, and R. L. Ehman, “Magnetic resonance elastography: Inversions in bounded media,” *Magn. Reson. Med.*, vol. 62, no. 6, pp. 1533–1542, Dec. 2009.

[12] G. E. Leclerc, L. Debernard, F. Foucart, L. Robert, K. M. Pelletier, F. Charleux, R. Ehman, M.-C. Ho Ba Tho, and S. F. Bensamoun, “Characterization of a hyper-viscoelastic phantom mimicking biological soft tissue using an abdominal pneumatic driver with magnetic resonance elastography (MRE),” *J. Biomech.*, vol. 45, no. 6, pp. 952–957, Apr. 2012.

[13] J. Oudry, T. Lynch, J. Vappou, L. Sandrin, and V. Miette, “Comparison of four different techniques to evaluate the elastic properties of phantom in elastography: is there a gold standard?,” *Phys. Med. Biol.*, vol. 59, no. 19, pp. 5775–5793, Oct. 2014.

[14] E. C. Qin, R. Sinkus, G. Geng, S. Cheng, M. Green, C. D. Rae, and L. E. Bilston, “Combining MR elastography and diffusion tensor imaging for the assessment of anisotropic mechanical properties: A phantom study,” *J. Magn. Reson. Imaging*, vol. 37, no. 1, pp. 217–226, Jan. 2013.

[15] M. A. Green, G. Geng, E. Qin, R. Sinkus, S. C. Gandevia, and L. E. Bilston, “Measuring anisotropic muscle stiffness properties using elastography,” *NMR Biomed.*, p. n/a–n/a, 2013.

[16] L. Debernard, G. E. Leclerc, L. Robert, F. Charleux, and S. F. Bensamoun, “In vivo characterization of the muscle viscoelasticity in passive and active conditions using multifrequency mr elastography,” *J. Musculoskelet. Res.*, vol. 16, no. 02, p. 1350008, Jun. 2013.

[17] L. Debernard, L. Robert, F. Charleux, and S. F. Bensamoun, “Analysis of thigh muscle stiffness from childhood to adulthood using magnetic resonance elastography (MRE) technique,” *Clin. Biomech.*, vol. 26, no. 8, pp. 836–840, Oct. 2011.

[18] S. F. Bensamoun, S. I. Ringleb, Q. Chen, R. L. Ehman, K.-N. An, and M. Brennan, “Thigh muscle stiffness assessed with magnetic resonance elastography in hyperthyroid patients before and after medical treatment,” *J. Magn. Reson. Imaging*, vol. 26, no. 3, pp. 708–713, Sep. 2007.

[19] Bensamoun S. F., Charleux F., and Themar-Noel C., “Elastic properties of skeletal muscle and subcutaneous tissues in Duchenne muscular dystrophy by magnetic resonance elastography (MRE): a feasibility study.,” *Innovation and Research in BioMedical engineering (IRBM).*, 2014.